ACS Medicinal Chemistry Letters

Letter

pubs.acs.org/acsmedchemlett

# Effects of the Arg-Pro and Gly-Gly-Nle Moieties on Melanocortin-1 Receptor Binding Affinities of α-MSH Peptides

Jianquan Yang,[†] Liqin Liu,[†] and Yubin Miao*[,†,‡,§]

[†]College of Pharmacy, [‡]Cancer Research and Treatment Center, [§]Department of Dermatology, University of New Mexico, Albuquerque, New Mexico 87131, United States

Supporting Information

**ABSTRACT:** The purpose of this study was to examine the effects of the -Arg-Pro- (RP) and -Gly-Gly-Nle- (GGNle) moieties on the melanoma targeting and clearance properties of $^{99m}$Tc-peptides. We synthesized four new peptides {Ac-GGNle-CCEHdFRWC-$NH_2$, Ac-GGNle-CCEHdFRWCRP-$NH_2$, Ac-CCEHdFRWC-NleGG-$NH_2$, and Ac-CCEHdFRWCRP-NleGG-$NH_2$} and determined their melanocortin-1 (MC1) receptor binding affinities in B16/F1 melanoma cells. Then we further examined the biodistribution properties of $^{99m}$Tc-Ac-GGNle-CCEHdFRWCRP-$NH_2$ and $^{99m}$Tc-Ac-CCEHdFRWCRP-NleGG-$NH_2$ in B16/F1 melanoma-bearing C57 mice. Overall, the -RP- moiety was critical for retaining low nanomolar MC1 receptor binding affinity. The deletion of the -RP- moiety dramatically reduced the receptor binding affinities of the peptides. The N-terminus was a better position than C-terminus for the -GGNle- moiety in retaining the lower renal and liver uptake. High melanoma uptake coupled with fast urinary clearance of $^{99m}$Tc-Ac-GGNle-CCEHdFRWCRP-$NH_2$ provided a new insight into the design of new α-melanocyte stimulating hormone (α-MSH) peptides.

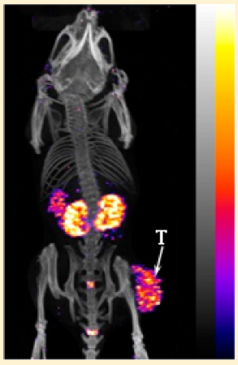


**KEYWORDS:** *Melanocortin-1 receptor, $^{99m}$Tc-labeled, alpha-MSH peptide, melanoma*

Over the past a few years, we and others have reported radiolabeled lactam bridge-cyclized alpha-melanocyte stimulating hormone (α-MSH) peptides to target melanocortin-1 (MC1) receptors for melanoma detection.[1−11] Specifically, we have developed two series of radiolabeled lactam bridge-cyclized α-MSH peptides building upon the CycMSH {c[Lys-Nle-Glu-His-DPhe-Arg-Trp-Gly-Arg-Pro-Val-Asp]} and $CycMSH_{hex}$ {c[Asp-His-DPhe-Arg-Trp-Lys]-$CONH_2$} constructs. Both DOTA (1,4,7,10-tetraazacyclododecane-1,4,7,10-tetraacetic acid) and NOTA (1,4,7-triazacyclononane-1,4,7-triacetic acid) were attached to the peptides for radiolabeling of $^{111}$In, $^{67}$Ga, and $^{64}$Cu for single photon emission computed tomography (SPECT) and positron emission tomography (PET) imaging of melanoma.[9−11] Among these radiolabeled peptides, $^{111}$In-DOTA-GGNle-$CycMSH_{hex}$ and $^{64}$Cu-NOTA-GGNle-$CycMSH_{hex}$ exhibited great potential as imaging probes for SPECT and PET imaging of melanoma due to their high melanoma uptake and fast urinary clearance.[9,10]

The unique structural features, such as the Asp-Lys lactam bridge and -GGNle- linker, contributed to the favorable melanoma targeting and clearance properties of $^{111}$In-DOTA-GGNle-$CycMSH_{hex}$ peptide. For instance, as compared to the CycMSH construct, the direct cyclization of the MC1 receptor binding motif {His-DPhe-Arg-Trp} by an Asp-Lys lactam bridge generated a smaller $CycMSH_{hex}$ moiety, which enhanced the melanoma uptake of $^{111}$In-DOTA-Nle-$CycMSH_{hex}$.[7] Furthermore, the introduction of -GG- linker dramatically reduced the renal and liver uptake of $^{111}$In-DOTA-GGNle-$CycMSH_{hex}$.[9] In an attempt to take advantage of the ideal imaging properties of $^{99m}$Tc (140 keV γ-photon and $T_{1/2}$ = 6 h), we developed several $^{99m}$Tc-labeled lactam bridge-cyclized α-MSH peptides via a bifunctional chelator approach. Specifically, we substituted DOTA/NOTA with hydrazinonicotinamide (HYNIC), mercaptoacetyltriglycine ($MAG_3$), and Ac-Cys-Gly-Gly-Gly ($AcCG_3$).[12] Both $MAG_3$ and $AcCG_3$ chelators directly yielded complexes with $^{99m}$Tc, whereas HYNIC generated a conjugate with $^{99m}$Tc in ethylenediaminediacetic acid (EDDA)/tricine solution. $^{99m}$Tc(EDDA)-HYNIC-GGNle-$CycMSH_{hex}$ exhibited higher melanoma uptake and faster urinary clearance than $^{99m}$Tc-$MAG_3$-GGNle-$CycMSH_{hex}$ and $^{99m}$Tc-$AcCG_3$-GGNle-$CycMSH_{hex}$ in B16/F1 melanoma-bearing C57 mice.[12]

An integration approach is another way to design $^{99m}$Tc-labeled cyclic α-MSH peptides.[13,14] For example, three cysteines were successfully utilized to generate the cyclic $^{99m}$Tc-($Arg^{11}$)CCMSH {$^{99m}$Tc-c[Cys-Cys-Glu-His-DPhe-Arg-Trp-Cys-Arg-Pro-Val]-$CONH_2$} peptide.[13] Interestingly, both $^{99m}$Tc-($Arg^{11}$)CCMSH and $^{99m}$Tc(EDDA)-HYNIC-GGNle-$CycMSH_{hex}$ exhibited comparable high melanoma uptake (11.16 ± 1.77 vs 13.23 ± 2.35% ID/g at 4 h postinjection) in B16/F1 melanoma-bearing C57 mice.[12,13] However, the chemical structures were quite different between $^{99m}$Tc-($Arg^{11}$)CCMSH and $^{99m}$Tc(EDDA)-HYNIC-GGNle-$CycMSH_{hex}$. A motif of -Arg-Pro-Val- (RPV) was attached to the C-terminus of ($Arg^{11}$)CCMSH peptide, whereas a -GGNle- linker was attached to the N-terminus of HYNIC-GGNle-$CycMSH_{hex}$ peptide. Thus, we were interested in examining whether and how the moieties of -RP- and -GGNle- could

**Received:** August 7, 2013
**Accepted:** September 4, 2013
**Published:** September 4, 2013

  

affect the melanoma targeting and clearance properties of $^{99m}$Tc-peptides in this study.

In consideration of the structural difference between $^{99m}$Tc-(Arg$^{11}$)CCMSH and $^{99m}$Tc(EDDA)-HYNIC-GGNle-CycMSH$_{hex}$, we designed four new peptides (namely, Ac-GGNle-CCEHdFRWC-NH$_2$, Ac-GGNle-CCEHdFRWCRP-NH$_2$, Ac-CCEHdFRWC-NleGG-NH$_2$, and Ac-CCEHdFRWCRP-NleGG-NH$_2$) to investigate whether and how the moieties of -RP- and -GGNle- could affect the melanoma targeting and clearance properties of $^{99m}$Tc-peptides. The schematic structures of the new peptides are presented in Figure 1. The peptides were synthesized and purified by reverse

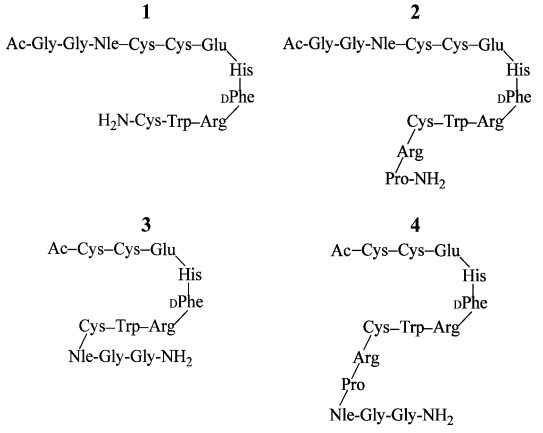


**Figure 1.** Schematic structures of Ac-GGNle-CCEHdFRWC-NH$_2$ (1), Ac-GGNle-CCEHdFRWCRP-NH$_2$ (2), Ac-CCEHdFRWC-NleGG-NH$_2$ (3), and Ac-CCEHdFRWCRP-NleGG-NH$_2$ (4).

phase-high performance liquid chromatography (RP-HPLC). The overall synthetic yields were 30% for all four peptides. The chemical purities of the peptides were greater than 95% after the HPLC purification. The peptide identities were confirmed by mass spectrometry. The measured molecular weight (MW) was 1351.5 for Ac-GGNle-CCEHdFRWC-NH$_2$, 1604.5 for Ac-GGNle-CCEHdFRWCRP-NH$_2$, 1351.5 for Ac-CCEHdFRWC-NleGG-NH$_2$, and 1604.5 for Ac-CCEHdFRWCRP-NleGG-NH$_2$. The measured MWs matched the calculated MWs.

The comparisons in receptor binding affinities between Ac-GGNle-CCEHdFRWC-NH$_2$/Ac-CCEHdFRWC-NleGG-NH$_2$ and Ac-GGNle-CCEHdFRWCRP-NH$_2$/Ac-CCEHdFRWCRP-NleGG-NH$_2$ can suggest whether the -RP- moiety is critical for MC1 receptor binding, whereas the comparisons in receptor binding affinities between Ac-GGNle-CCEHdFRWC-NH$_2$/Ac-GGNle-CCEHdFRWCRP-NH$_2$ and Ac-CCEHdFRWC-NleGG-NH$_2$/Ac-CCEHdFRWCRP-NleGG-NH$_2$ can indicate which terminus (N- or C-terminus) is better for the -GGNle- moiety in retaining stronger MC1 receptor binding. Thus, we determined the MC1 receptor binding affinities of these four peptides in B16/F1 melanoma cells. The competitive binding curves of the peptides are shown in Figure 2. The IC$_{50}$ value was 27.1 ± 5.5 nM for Ac-GGNle-CCEHdFRWC-NH$_2$, 2.0 ± 0.4 nM for Ac-GGNle-CCEHdFRWCRP-NH$_2$, 70.9 ± 18.9 nM for Ac-CCEHdFRWC-NleGG-NH$_2$, and 4.1 ± 0.6 nM for Ac-CCEHdFRWCRP-NleGG-NH$_2$, respectively.

The receptor binding results indicated that the -RP- moiety was critical for retaining low nanomolar MC1 receptor binding affinities of the peptides in B16/F1 melanoma cells. The deletion of the -RP- moiety dramatically reduced the receptor binding affinities of the peptides. For instance, Ac-GGNle-

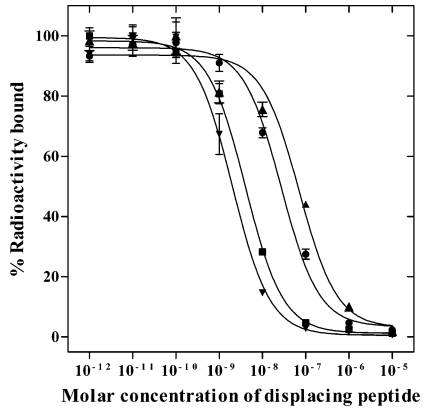


**Figure 2.** Competitive binding curves of Ac-GGNle-CCEHdFRWC-NH$_2$ (●), Ac-GGNle-CCEHdFRWCRP-NH$_2$ (▼), Ac-CCEHdFRWC-NleGG-NH$_2$ (▲), and Ac-CCEHdFRWCRP-NleGG-NH$_2$ (■) in B16/F1 melanoma cells.

CCEHdFRWCRP-NH$_2$ and Ac-CCEHdFRWCRP-NleGG-NH$_2$ displayed stronger MC1 receptor binding affinities than Ac-GGNle-CCEHdFRWC-NH$_2$ and Ac-CCEHdFRWC-NleGG-NH$_2$. The IC$_{50}$ value of Ac-GGNle-CCEHdFRWC-NH$_2$ was 13.6 times the IC$_{50}$ value of Ac-GGNle-CCEHdFRWCRP-NH$_2$, whereas the IC$_{50}$ value of Ac-CCEHdFRWC-NleGG-NH$_2$ was 17.3 times the IC$_{50}$ value of Ac-CCEHdFRWC-NleGG-NH$_2$. Meanwhile, the N-terminus was better than C-terminus for the -GGNle- moiety for stronger MC1 receptor binding. The IC$_{50}$ value of Ac-CCEHdFRWCRP-NleGG-NH$_2$ was 2.1 times the IC$_{50}$ value of Ac-GGNle-CCEHdFRWCRP-NH$_2$, whereas the IC$_{50}$ value of Ac-CCEHdFRWC-NleGG-NH$_2$ was 2.6 times the IC$_{50}$ value of Ac-CCEHdFRWC-NleGG-NH$_2$. Thus, we further radiolabeled Ac-GGNle-CCEHdFRWCRP-NH$_2$ and Ac-CCEHdFRWCRP-NleGG-NH$_2$ with $^{99m}$Tc.

Both Ac-GGNle-CCEHdFRWCRP-NH$_2$ and Ac-CCEHdFRWCRP-NleGG-NH$_2$ have three cysteines that can directly form a complex with $^{99m}$Tc, as well as can simultaneously cyclize the peptide during the radiolabeling of $^{99m}$Tc. Ac-GGNle-CCEHdFRWCRP-NH$_2$ and Ac-CCEHdFRWCRP-NleGG-NH$_2$ were readily labeled with $^{99m}$Tc with greater than 95% radiolabeling yields. Both $^{99m}$Tc-peptides were purified and separated from their excess nonlabeled peptides by RP-HPLC. The retention times of $^{99m}$Tc-Ac-GGNle-CCEHdFRWCRP-NH$_2$ and $^{99m}$Tc-Ac-CCEHdFRWCRP-NleGG-NH$_2$ were 14.8 and 15.0 min, respectively. The specific activities of both $^{99m}$Tc-peptides were 1.20 × 10$^{10}$ MBq/g.

The melanoma targeting and pharmacokinetic properties of $^{99m}$Tc-Ac-GGNle-CCEHdFRWCRP-NH$_2$ and $^{99m}$Tc-Ac-CCEHdFRWCRP-NleGG-NH$_2$ are shown in Tables 1 and 2. $^{99m}$Tc-Ac-GGNle-CCEHdFRWCRP-NH$_2$ displayed slightly higher but comparable melanoma uptake as $^{99m}$Tc-Ac-CCEHdFRWCRP-NleGG-NH$_2$ in B16/F1 melanoma-bearing C57 mice. However, the tumor uptake pattern was different between $^{99m}$Tc-Ac-GGNle-CCEHdFRWCRP-NH$_2$ and $^{99m}$Tc-Ac-CCEHdFRWCRP-NleGG-NH$_2$. $^{99m}$Tc-Ac-GGNle-CCEHdFRWCRP-NH$_2$ exhibited its highest tumor uptake of 10.54 ± 1.6% ID/g at 2 h postinjection, whereas $^{99m}$Tc-Ac-CCEHdFRWCRP-NleGG-NH$_2$ reached its highest tumor uptake of 8.08 ± 1.61% ID/g at 30 min postinjection. The tumor uptake values gradually decreased to 4.40 ± 0.91 and 3.88 ± 0.66% ID/g by 24 h postinjection. The tumor blocking


dx.doi.org/10.1021/ml400309u | ACS Med. Chem. Lett. 2013, 4, 1000−1004

**Table 1. Biodistribution of $^{99m}$Tc-Ac-GGNle-CCEHdFRWCRP-$NH_2$ in B16/F1 Melanoma-Bearing C57 Mice; the Data Were Presented As Percent Injected Dose/Gram or As Percent Injected Dose (Mean ± SD, $n$ = 5)**

| tissues | 0.5 h | 2 h | 4 h | 24 h | 2 h NDP blockade |
|---|---|---|---|---|---|
| Percent Injected Dose/Gram (%ID/g) | | | | | |
| tumor | 8.90 ± 1.13 | 10.54 ± 1.60 | 9.76 ± 1.38 | 4.40 ± 0.91 | 2.05 ± 0.96* |
| brain | 0.16 ± 0.04 | 0.05 ± 0.01 | 0.04 ± 0.02 | 0.02 ± 0.02 | 0.04 ± 0.02 |
| blood | 2.88 ± 1.83 | 0.76 ± 0.84 | 0.25 ± 0.26 | 0.08 ± 0.09 | 0.61 ± 0.57 |
| heart | 2.14 ± 0.28 | 0.55 ± 0.22 | 0.32 ± 0.07 | 0.13 ± 0.12 | 0.59 ± 0.2 |
| lung | 6.53 ± 2.47 | 1.74 ± 0.88 | 0.68 ± 0.14 | 0.14 ± 0.05 | 1.76 ± 0.62 |
| liver | 4.34 ± 0.44 | 3.19 ± 0.47 | 2.67 ± 0.61 | 0.67 ± 0.20 | 2.70 ± 1.04 |
| spleen | 3.50 ± 2.39 | 3.17 ± 2.24 | 2.20 ± 0.60 | 2.77 ± 1.42 | 2.36 ± 2.37 |
| stomach | 3.17 ± 1.07 | 1.67 ± 0.16 | 1.18 ± 0.07 | 0.33 ± 0.12 | 0.66 ± 0.31 |
| kidneys | 13.95 ± 4.57 | 11.45 ± 2.30 | 10.50 ± 1.27 | 1.24 ± 0.28 | 13.15 ± 3.98 |
| muscle | 0.94 ± 0.24 | 0.21 ± 0.24 | 0.12 ± 0.04 | 0.06 ± 0.04 | 0.14 ± 0.05 |
| pancreas | 0.84 ± 0.29 | 0.28 ± 0.09 | 0.15 ± 0.04 | 0.12 ± 0.06 | 0.32 ± 0.12 |
| bone | 2.30 ± 2.61 | 0.82 ± 0.30 | 0.31 ± 0.04 | 0.17 ± 0.12 | 0.91 ± 0.17 |
| skin | 4.69 ± 1.00 | 1.07 ± 0.37 | 0.72 ± 0.10 | 0.29 ± 0.12 | 1.17 ± 0.63 |
| Percent Injected Dose (%ID) | | | | | |
| intestines | 2.41 ± 0.15 | 2.74 ± 1.34 | 1.94 ± 0.38 | 1.38 ± 0.88 | 1.81 ± 0.67 |
| urine | 51.74 ± 5.26 | 79.15 ± 4.43 | 79.78 ± 5.11 | 93.28 ± 2.36 | 81.22 ± 6.79 |

*$p$ < 0.05 for determining the significance of differences in tumor and kidney uptake between $^{99m}$Tc-Ac-GGNle-CCEHdFRWCRP-$NH_2$ with or without NDP-MSH peptide blockade.

**Table 2. Biodistribution of $^{99m}$Tc-Ac-CCEHdFRWCRP-NleGG-$NH_2$ in B16/F1 Melanoma-Bearing C57 Mice; the Data Were Presented As Percent Injected Dose/Gram or As Percent Injected Dose (Mean ± SD, $n$ = 5)**

| tissues | 0.5 h | 2 h | 4 h | 24 h | 2 h NDP blockade |
|---|---|---|---|---|---|
| Percent Injected Dose/Gram (%ID/g) | | | | | |
| tumor | 8.08 ± 1.61 | 7.33 ± 1.72 | 6.74 ± 1.97 | 3.88 ± 0.66 | 2.83 ± 1.04* |
| brain | 0.23 ± 0.01 | 0.05 ± 0.01 | 0.04 ± 0.01 | 0.01 ± 0.01 | 0.04 ± 0.02 |
| blood | 4.37 ± 3.11 | 1.20 ± 0.80 | 0.73 ± 0.52 | 0.17 ± 0.21 | 1.12 ± 0.29 |
| heart | 3.02 ± 0.43 | 0.82 ± 0.23 | 0.61 ± 0.14 | 0.06 ± 0.04 | 1.46 ± 1.36 |
| lung | 6.88 ± 0.49 | 1.31 ± 0.63 | 0.84 ± 0.23 | 0.27 ± 0.11 | 3.18 ± 2.73 |
| liver | 10.37 ± 0.93 | 6.32 ± 0.76 | 5.27 ± 0.29 | 0.94 ± 0.21 | 7.18 ± 2.17 |
| spleen | 3.46 ± 2.21 | 2.17 ± 0.59 | 1.91 ± 1.07 | 0.58 ± 0.36 | 1.72 ± 1.14 |
| stomach | 9.40 ± 1.83 | 4.42 ± 1.14 | 2.99 ± 1.42 | 1.34 ± 1.57 | 3.35 ± 1.32 |
| kidneys | 28.31 ± 6.41 | 29.65 ± 4.28 | 24.86 ± 3.54 | 7.40 ± 2.63 | 30.19 ± 1.00 |
| muscle | 0.78 ± 0.39 | 0.14 ± 0.03 | 0.60 ± 0.33 | 0.10 ± 0.08 | 0.31 ± 0.38 |
| pancreas | 1.49 ± 0.27 | 0.52 ± 0.19 | 0.23 ± 0.12 | 0.09 ± 0.06 | 0.52 ± 0.50 |
| bone | 1.68 ± 0.22 | 0.54 ± 0.17 | 0.46 ± 0.21 | 0.30 ± 0.20 | 0.48 ± 0.13 |
| skin | 4.34 ± 0.51 | 0.96 ± 0.17 | 0.10 ± 0.03 | 0.25 ± 0.09 | 0.85 ± 0.41 |
| Percent Injected Dose (%ID) | | | | | |
| intestines | 6.10 ± 0.42 | 11.07 ± 1.41 | 12.25 ± 1.84 | 3.48 ± 0.87 | 9.55 ± 0.68 |
| urine | 35.43 ± 3.76 | 59.57 ± 4.01 | 66.97 ± 2.69 | 89.46 ± 2.98 | 67.67 ± 2.74 |

*$p$ < 0.05 for determining the significance of differences in tumor and kidney uptake between $^{99m}$Tc-Ac-CCEHdFRWCRP-NleGG-$NH_2$ with or without NDP-MSH peptide blockade.

studies (Tables 1 and 2) demonstrated that coinjection of 10 μg (6.1 nM) of nonradiolabeled NDP-MSH with $^{99m}$Tc-Ac-GGNle-CCEHdFRWCRP-$NH_2$ or $^{99m}$Tc-Ac-CCEHdFRWCRP-NleGG-$NH_2$ decreased their tumor uptake values to 2.05 ± 0.96 and 2.83 ± 1.04% ID/g at 2 h postinjection, demonstrating that the tumor uptake was MC1 receptor-mediated.

Interestingly, despite the similar tumor uptake, $^{99m}$Tc-Ac-GGNle-CCEHdFRWCRP-$NH_2$ exhibited lower renal uptake than $^{99m}$Tc-Ac-CCEHdFRWCRP-NleGG-$NH_2$ at 0.5, 2, 4, and 24 h postinjection. The renal uptake of $^{99m}$Tc-Ac-GGNle-CCEHdFRWCRP-$NH_2$ was 49, 37, 42 and 17% of the renal uptake of $^{99m}$Tc-Ac-CCEHdFRWCR-NleGG-$NH_2$ at 0.5, 2, 4, and 24 h postinjection, respectively. The renal uptake values of $^{99m}$Tc-Ac-GGNle-CCEHdFRWCRP-$NH_2$ and $^{99m}$Tc-Ac-CCEHdFRWCRP-NleGG-$NH_2$ were 11.45 ± 2.30 and 29.65 ± 4.28% ID/g at 2 h post injection and decreased to 1.24 ± 0.28 and 7.40 ± 2.63% ID/g at 24 h postinjection, respectively. Meanwhile, $^{99m}$Tc-Ac-GGNle-CCEHdFRWCRP-$NH_2$ exhibited lower liver uptake than $^{99m}$Tc-Ac-CCEHdFRWCRP-NleGG-$NH_2$ at 0.5, 2, 4, and 24 h postinjection. The liver uptake of $^{99m}$Tc-Ac-GGNle-CCEHdFRWCRP-$NH_2$ was 42, 50, 51, and 71% of the liver uptake of $^{99m}$Tc-Ac-CCEHdFRWCRP-NleGG-$NH_2$ at 0.5, 2, 4, and 24 h post-injection, respectively. The liver uptake values of $^{99m}$Tc-Ac-GGNle-CCEHdFRWCRP-$NH_2$ and $^{99m}$Tc-Ac-CCEHdFRWCRP-NleGG-$NH_2$ were 3.19 ± 0.47 and 6.32 ± 0.76% ID/g at 2 h post injection and decreased to 0.67 ± 0.20 and 0.94 ± 0.21% ID/g at 24 h postinjection, respectively. The differences in renal and liver uptake between $^{99m}$Tc-Ac-GGNle-CCEHdFRWCRP-$NH_2$ and


dx.doi.org/10.1021/ml400309u | ACS Med. Chem. Lett. 2013, 4, 1000−1004

$^{99m}$Tc-Ac-CCEHdFRWCRP-NleGG-$NH_2$ suggested that the N-terminus was a better position than the C-terminus for the -GGNle- moiety in retaining the lower renal and liver uptake. $^{99m}$Tc-Ac-GGNle-CCEHdFRWCRP-$NH_2$ exhibited faster whole-body clearance than $^{99m}$Tc-Ac-CCEHdFRWCRP-NleGG-$NH_2$. Approximately 79% of $^{99m}$Tc-Ac-GGNle-CCEHdFRWCRP-$NH_2$ radioactivity and 60% of $^{99m}$Tc-Ac-CCEHdFRWCRP-NleGG-$NH_2$ radioactivity cleared through the urinary system by 2 h postinjection (Tables 1 and 2). At 24 h postinjection, 93% of $^{99m}$Tc-Ac-GGNle-CCEHdFRWCRP-$NH_2$ and 89% of $^{99m}$Tc-Ac-CCEHdFRWCRP-NleGG-$NH_2$ activity cleared out the body. Since $^{99m}$Tc-Ac-GGNle-CCEHdFRWCRP-$NH_2$ exhibited more favorable tumor targeting and clearance properties than $^{99m}$Tc-Ac-CCEHdFRWCRP-NleGG-$NH_2$, we further examined the melanoma imaging property of $^{99m}$Tc-Ac-GGNle-CCEHdFRWCRP-$NH_2$. Whole-body SPECT/CT image of $^{99m}$Tc-Ac-GGNle-CCEHdFRWCRP-$NH_2$ is presented in Figure 3. Flank B16/F1 melanoma lesions were clearly visualized by SPECT using $^{99m}$Tc-Ac-GGNle-CCEHdFRWCRP-$NH_2$ as an imaging probe. Recent publications[15,16] have described proliferative and invasive melanoma cells and addressed the heterogeneity issue in melanoma. The SPECT image showed heterogeneous distribution of radioactivity in melanoma, which was likely related to the heterogeneous expressions of MC1 receptors on melanoma cells. Furthermore, we determined the urinary metabolites of $^{99m}$Tc-Ac-GGNle-CCEHdFRWCRP-$NH_2$ at 2 h postinjection. The urinary metabolites of $^{99m}$Tc-Ac-GGNle-CCEHdFRWCRP-$NH_2$ are shown in Figure 4. Approximately 52% of $^{99m}$Tc-Ac-GGNle-CCEHdFRWCRP-$NH_2$ remained intact in the urine at 2 h postinjection, while 48% of $^{99m}$Tc-Ac-GGNle-CCEHdFRWCRP-$NH_2$ was transformed to a more hydrophobic compound.

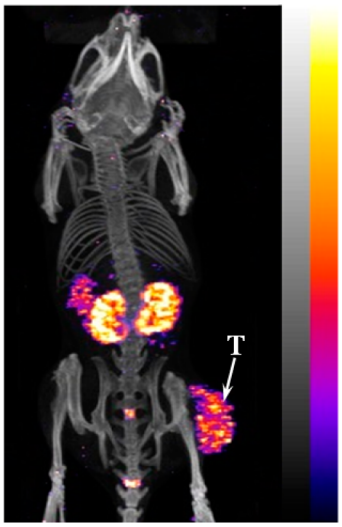


**Figure 3.** Representative whole-body SPECT/CT image of $^{99m}$Tc-Ac-GGNle-CCEHdFRWCRP-$NH_2$ in a B16/F1 melanoma-bearing C57 mouse at 2 h postinjection. The tumor lesions (T) are highlighted with an arrow on the image.

In summary, four new peptides were evaluated to examine the effects of the -RP- and -GGNle- moieties on the melanoma targeting and clearance properties of $^{99m}$Tc-peptides. The -RP- moiety was critical for retaining low nanomolar MC1 receptor binding affinity. The deletion of the -RP- moiety dramatically reduced the receptor binding affinities of the peptides. The N-terminus was a better position than C-terminus for the -GGNle- moiety in retaining the lower renal and liver uptake. High melanoma uptake coupled with fast urinary clearance of $^{99m}$Tc-Ac-GGNle-CCEHdFRWCRP-$NH_2$ provided a new insight into the design of new $\alpha$-MSH peptides.

## ■ ASSOCIATED CONTENT

### Ⓢ Supporting Information

Experimental details for peptide synthesis, in vitro competitive binding assay, radiolabeling, biodistribution and imaging studies, and urinary metabolites analysis. This material is available free of charge via the Internet at http://pubs.acs.org.

## ■ AUTHOR INFORMATION

### Corresponding Author

*(Y.M.) E-mail: ymiao@salud.unm.edu. Phone: (505) 925-4437. Fax: (505) 272-6749.

### Funding

This work was supported in part by the NIH grant NM-INBRE P20RR016480/P20GM103451 and UNM RAC Award. The images were generated by the KUSAIR established with funding from the W. M. Keck Foundation and the UNM Cancer Research and Treatment Center (NIH P30 CA118100).

### Notes

The authors declare no competing financial interest.

## ■ ACKNOWLEDGMENTS

We appreciate Dr. Fabio Gallazzi for his technical assistance.

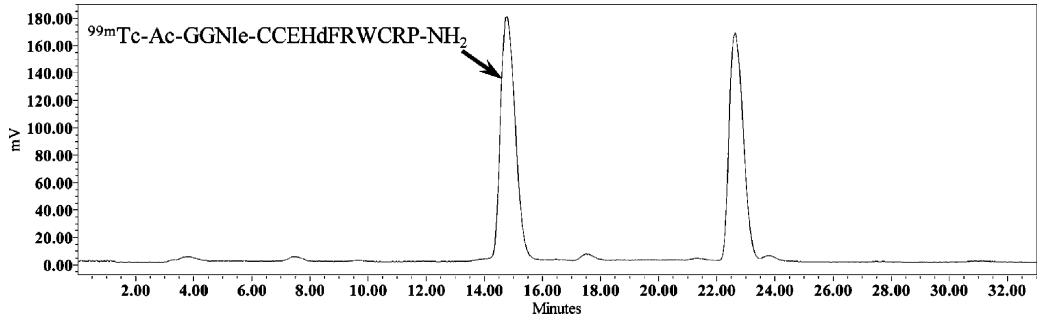


**Figure 4.** Radioactive HPLC profile of a urine sample of a B16/F1 melanoma-bearing C57 mouse at 2 h postinjection of $^{99m}$Tc-Ac-GGNle-CCEHdFRWCRP-$NH_2$. The arrow indicates the retention time (14.8 min) of the original compound of $^{99m}$Tc-Ac-GGNle-CCEHdFRWCRP-$NH_2$ prior to the tail vein injection.

## REFERENCES


(1) Miao, Y.; Gallazzi, F.; Guo, H.; Quinn, T. P. $^{111}$In-labeled lactam bridge-cyclized alpha-melanocyte stimulating hormone peptide analogues for melanoma imaging. *Bioconjugate Chem.* **2008**, *19*, 539−547.

(2) Raposinho, P. D.; Correia, J. D.; Alves, S.; Botelho, M. F.; Santos, A. C.; Santos, I. A $^{99m}$Tc(CO)$_3$-labeled pyrazolyl-$\alpha$-melanocyte-stimulating hormone analog conjugate for melanoma targeting. *Nucl. Med. Biol.* **2008**, *35*, 91−99.

(3) Guo, H.; Shenoy, N.; Gershman, B. M.; Yang, J.; Sklar, L. A.; Miao, Y. Metastatic melanoma imaging with an $^{111}$In-labeled lactam bridge-cyclized alpha-melanocyte-stimulating hormone peptide. *Nucl. Med. Biol.* **2009**, *36*, 267−276.

(4) Guo, H.; Yang, J.; Gallazzi, F.; Prossnitz, E. R.; Sklar, L. A.; Miao, Y. Effect of DOTA position on melanoma targeting and pharmacokinetic properties of $^{111}$In-labeled lactam bridge-cyclized $\alpha$-melanocyte stimulating hormone peptide. *Bioconjugate Chem.* **2009**, *20*, 2162−2168.

(5) Raposinho, P. D.; Xavier, C.; Correia, J. D.; Falcao, S.; Gomes, P.; Santos, I. Melanoma targeting with alpha-melanocyte stimulating hormone analogs labeled with fac-[$^{99m}$Tc(CO)$_3$]$^+$: effect of cyclization on tumor-seeking properties. *J. Biol. Inorg. Chem.* **2008**, *13*, 449−459.

(6) Guo, H.; Yang, J.; Shenoy, N.; Miao, Y. Gallium-67-labeled lactam bridge-cyclized alpha-melanocyte stimulating hormone peptide for primary and metastatic melanoma imaging. *Bioconjugate Chem.* **2009**, *20*, 2356−2363.

(7) Guo, H.; Yang, J.; Gallazzi, F.; Miao, Y. Reduction of the ring size of radiolabeled lactam bridge-cyclized alpha-MSH peptide resulting in enhanced melanoma uptake. *J. Nucl. Med.* **2010**, *51*, 418−426.

(8) Morais, M.; Oliveira, B. L.; Correia, J. D.; Oliveira, M. C.; Jiménez, M. A.; Santos, I.; Raposinho, P. D. Influence of the bifunctional chelator on the pharmacokinetic properties of $^{99m}$Tc-(CO)$_3$-labeled cyclic $\alpha$-melanocyte stimulating hormone analog. *J. Med. Chem.* **2013**, *56*, 1961−1973.

(9) Guo, H.; Yang, J.; Gallazzi, F.; Miao, Y. Effects of the amino acid linkers on melanoma-targeting and pharmacokinetic properties of indium-111-labeled lactam bridge-cyclized $\alpha$-MSH peptides. *J. Nucl. Med.* **2011**, *52*, 608−616.

(10) Guo, H.; Miao, Y. Cu-64-labeled lactam bridge-cyclized alpha-MSH peptides for PET imaging of melanoma. *Mol. Pharmaceutics* **2012**, *9*, 2322−2330.

(11) Guo, H.; Gallazzi, F.; Miao, Y. Ga-67-labeled lactam bridge-cyclized alpha-MSH peptides with enhanced melanoma uptake and reduced renal uptake. *Bioconjugate Chem.* **2012**, *23*, 1341−1348.

(12) Guo, H.; Gallazzi, F.; Miao, Y. Design and evaluation of new Tc-99m-labeled lactam bridge-cyclized alpha-MSH peptides for melanoma imaging. *Mol. Pharmaceutics* **2013**, *10*, 1400−1408.

(13) Miao, Y.; Benwell, K.; Quinn, T. P. $^{99m}$Tc- and $^{111}$In-labeled alpha-melanocyte-stimulating hormone peptides as imaging probes for primary and pulmonary metastatic melanoma detection. *J. Nucl. Med.* **2007**, *48*, 73−80.

(14) Chen, J.; Cheng, Z.; Hoffman, T. J.; Jurisson, S. S.; Quinn, T. P. Melanoma-targeting properties of $^{99m}$technetium-labeled cyclic alpha-melanocyte-stimulating hormone peptide analogues. *Cancer Res.* **2000**, *60*, 5649−5658.

(15) Hoek, K. S.; Eichhoff, O. M.; Schlegel, N. C.; Döbbeling, U.; Kobert, N.; Schaerer, L.; Hemmi, S.; Dummer, R. In vivo switching of human melanoma cells between proliferative and invasive states. *Cancer Res.* **2008**, *68*, 650−656.

(16) Hoek, K. S. DNA microarray analyses of melanoma gene expression: a decade in the mines. *Pigment Cell Res.* **2007**, *20*, 466−484.